Inorganic Chemistry

pubs.acs.org/IC
Article

Tailor-Made Synthesis of Hydrosilanols, Hydrosiloxanes, and Silanediols Catalyzed by di-Silyl Rhodium(III) and Iridium(III) Complexes

Unai Prieto-Pascual, Antonio Rodríguez-Diéguez, Zoraida Freixa,* and Miguel A. Huertos*

Cite This: *Inorg. Chem.* 2023, 62, 3095−3105
Read Online

ABSTRACT: Siloxanes and silanols containing Si−H units are important building blocks for the synthesis of functionalized siloxane materials, and their synthesis is a current challenge. Herein, we report the selective synthesis of hydrosilanols, hydrosiloxanes, and silanodiols depending on the nature of the catalysts and the silane used. Two neutral ({MCl[$SiMe_2$(*o*-$C_6H_4PPh_2$)]$_2$}; M = Rh, Ir) and two cationic ({M[$SiMe_2$(*o*-$C_6H_4PPh_2$)]$_2$(NCMe)}[$BAr^F{}_4$]; M = Rh, Ir) have been synthesized and their catalytic behavior toward hydrolysis of secondary silanes has been described. Using the iridium complexes as precatalysts and diphenylsilane as a substrate, the product obtained is diphenylsilanediol. When rhodium complexes are used as precatalysts, it is possible to selectively obtain silanediol, hydrosilanol, and hydrosiloxane depending on the catalysts (neutral or cationic) and the silane substituents.

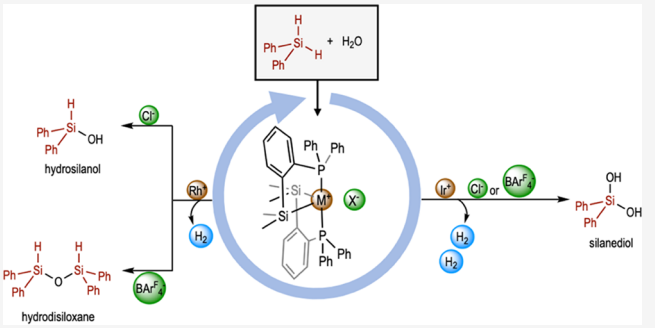

INTRODUCTION

Silicones (oligo- and polysiloxane materials) are an important class of inorganic materials that find many industrial applications due to their outstanding physicochemical properties (thermal and light stability and resistance to water and oxidation).[1,2] There are well-known methods for the synthesis of siloxane materials. The most used to date are the ring-opening polymerization of cyclic siloxanes and sol−gel processes (hydrolytic condensation of chlorosilanes (Cl−Si) or alkoxysilanes (RO−Si)).[3]

Nowadays, one of the main challenges in the synthesis of siloxane materials is to find methods to construct highly functionalized siloxanes with a well-defined structure. This could be achieved by using siloxanes, alkoxysilanes, and silanols, containing Si−H moieties as building blocks. Si−H bond is one of the most useful functional groups in silicon chemistry, and there are a large number of well-known reactions to transform this functional group (e.g., *via* hydrosilylation reactions).[4,5] Moreover, siloxanes with Si−H moieties are also interesting molecules to functionalize organic and inorganic compounds.[6] Silanols, besides being used in the production of silicon-based polymers,[7] are important intermediates in organic synthesis (e.g., an efficient organic donor in metal-catalyzed cross-coupling).[8]

In 2010, Kuroda et al. reported a pioneering study on the selective synthesis of hydrosiloxanes through a cross-coupling type reaction catalyzed by $BiCl_3$. Unfortunately, the product could not be effectively separated from the catalyst.[9] Recently, more effective synthetic catalytic methods for the formation of hydrosiloxanes have been reported by reacting dihydrosilanes with silanols catalyzed by gold,[10] cobalt,[11] Fe,[12] or main-group species.[13] Alternatively, they can be obtained by dealcoholization reaction between silanols and alkoxyhydrosilanes without the use of catalyst or additives.[14]

In the case of the synthesis of silanols,[15] there are well-established methods based on the hydrolysis of chlorosilanes,[16] oxidation of hydrosilanes using strong oxidants,[17] H_2O_2[18] or O_2[19] and the metal catalytic hydrolytic oxidation of hydrosilanes with water (also known as hydrolysis of silanes).[20] Reusable heterogeneous catalysts have also been used in the hydrolysis of silanes.[21] The importance of the hydrolysis of silanes lies in the atom efficiency of this process. Recent studies have shown that silanols can also be obtained by electrochemical hydrolysis[22] and enzymatic oxidation[23] of hydrosilanes.

Focusing on the synthesis of hydrosilanols through metal-catalyzed oxidation of dihydrosilanes using H_2O, few selective methods have been reported to date.[24] The problem is the presence of two reactive Si−H and the competitive

Received: November 9, 2022
Published: February 9, 2023

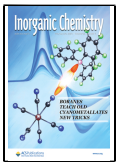

https://doi.org/10.1021/acs.inorgchem.2c03953
Inorg. Chem. 2023, 62, 3095−3105

condensation reactions.[20f,g,m,n] Thus, the hydrolysis of dihydrosilanes might lead to the formation of several products, as shown in Scheme 1, or mixtures thereof.

Scheme 1. Hydrolysis of Dihydrosilanes and Possible Reaction Products

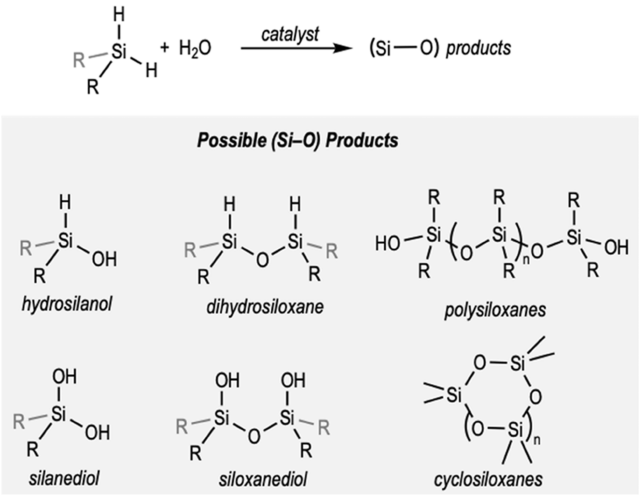

Herein, we report the catalytic activity of two neutral ($\{MCl[SiMe_2(o\text{-}C_6H_4PPh_2)]_2\}$; M = Rh, Ir) and two cationic ($\{M[SiMe_2(o\text{-}C_6H_4PPh_2)]_2(NCMe)\}[BAr^F{}_4]$; M = Rh, Ir) complexes in the hydrolysis of dihydrosilanes. The difference in the structure of each complex, together with the nature of the dihydrosilane used, allowed us to selectively synthesize different types of related Si−O products (Scheme 1).

RESULTS AND DISCUSSION

Synthesis and Characterization of Neutral and Cationic P,Si-Complexes. Reaction of $[RhCl(coe)_2]_2$ with 4 equiv of the proligand $[Si(H)Me_2(o\text{-}C_6H_4PPh_2)]$ in CH_2Cl_2 at room temperature afforded, after 1 h, the air-stable compound $\{RhCl[SiMe_2(o\text{-}C_6H_4PPh_2)]_2\}$ (**1** in Scheme 2)

Scheme 2. Synthesis of Complexes 1 and 2

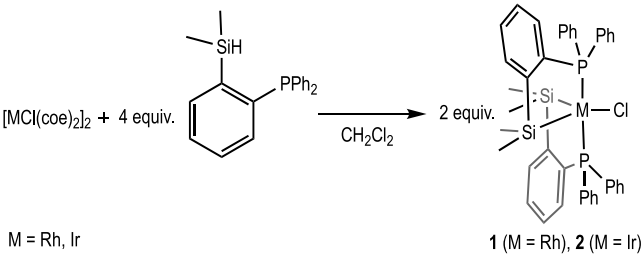

in good yield (92%), which was characterized in solution by NMR spectroscopy. In the ^1H NMR spectrum, two singlets are observed for the Si−CH_3 groups (δ −0.07 and δ −0.43) due to the nonequivalence of the methyl groups on each silicon atom upon coordination to rhodium, as previously observed in a related compound.[25] The $^{31}P\{^1H\}$ NMR spectrum shows a unique signal as a doublet at δ 55.6 ($J_{Rh\text{-}P}$ = 120 Hz), which indicates that both ligands are equivalent in solution. An isoelectronic iridium complex, $\{IrCl[SiMe_2(o\text{-}C_6H_4PPh_2)]_2\}$ (**2** in Scheme 2), was synthesized by reaction of $[IrCl(coe)_2]_2$ with 4 equiv of $[Si(H)Me_2(o\text{-}C_6H_4PPh_2)]$ under the same reaction conditions (78% yield). The ^1H NMR spectroscopic pattern of complex **2** in solution is similar to that observed for complex **1** (see Experimental Section and Supporting Information, SI for more details). The $^{31}P\{^1H\}$ NMR shows a singlet at δ 54.4 that indicates equivalent triarylphosphine groups.

Compounds **1** and **2** were also characterized by single-crystal X-ray structural determination (Figure 1). The resulting molecular structures are in good agreement with the structures deduced from the spectroscopic data in solution. In the solid state, the geometry about the Rh(III) center in complex **1** can be described as a distorted trigonal bipyramid with the apical positions occupied by the phosphorous atoms (P1 and P1_i) and the equatorial positions occupied by the silicon (Si1 and Si1_i) and the chlorine atoms. The rhodium atom is included in the plane Si1Cl1Si1_i. The sum of the three angles (Cl1−Rh1−Si1, Si1−Rh1−Si1_i, and Si1_i−Rh1−Cl1) being 360° and the P1−Rh1−P1_i angle of 177.43(3)° suggest this geometry. Molecular structure of complex **2**, in the solid state, is isostructural to that described for compound **1** (Figure 1b).

Treatment of complexes **1** and **2** with an equimolar amount of $NaBAr^F{}_4$ in CH_2Cl_2 and in the presence of a small amount of MeCN yielded the Rh(III) cationic complex $\{Rh[SiMe_2(o\text{-}C_6H_4PPh_2)]_2(NCMe)\}[BAr^F{}_4]$ (**1**[**BAr**$^F{}_4$]) and a similar cationic complex with two acetonitrile molecules coordinated to the metal center, $\{Ir[SiMe_2(o\text{-}C_6H_4PPh_2)]_2(NCMe)_2\}[BAr_4{}^F]$ (**2**[**BAr**$^F{}_4$]), respectively (Scheme 3).

Compounds **1**[**BAr**$^F{}_4$] and **2**[**BAr**$^F{}_4$] were characterized in solution by NMR spectroscopy (see Experimental Section and SI for more details). Both complexes showed in the ^1H NMR spectrum two different signals for the Si−CH_3 groups (δ 0.04 and δ −0.32 for **1**[**BAr**$^F{}_4$]; δ −0.10 and δ −0.26 for **2**[**BAr**$^F{}_4$]). The signals assigned to coordinated MeCN were observed at 1.78 ppm (integrating by 3H) in the case of **1**[**BAr**$^F{}_4$] and at 1.48 (integrating by 6H) in the case of **2**[**BAr**$^F{}_4$]. The equivalence of both phosphines in solution is confirmed by the presence of only one signal in the $^{31}P\{^1H\}$ NMR spectra. They appear as a doublet at 55.5 ppm {$J_{Rh\text{-}P}$ = 120 Hz} ppm for **1**[**BAr**$^F{}_4$] and a singlet at 38.1 ppm for **2**[**BAr**$^F{}_4$]. The spectroscopic data were consistent with a pentacoordinated Rh(III) complex in **1**[**BAr**$^F{}_4$] and a pseudo-octahedral Ir(III) structure in the case of **2**[**BAr**$^F{}_4$], as proposed in Scheme 3.

These structures were confirmed by X-ray diffraction (Figure 2). Figure 2a shows the solid-state structure of **1**[**BAr**$^F{}_4$]. The formally Rh(III) center adopts a square pyramid geometry with one of the silicon atoms (Si1) located on the apical position. The plane defined by the other silicon atom (Si2), the two phosphorous atoms, and the acetonitrile ligand (Si2P1P2N1), where is included the rhodium atom, forms the base of the pyramid. The sum of the four angles (Si2−Rh1−P1, P1−Rh1−N1, N1−Rh1−P2, and P2−Rh1−Si2) being 360° suggests this geometry. It is important to note that in solution, both SiP chelate ligands are equivalent. This could be due to a rapid interchange of MeCN located trans to Si2 to be placed trans to Si1.

The solid-state structure of **2**[**BAr**$_4{}^F$] is showed in Figure 2b. The resulting molecular structure agrees with the structure deduced from the spectroscopic data in solution. The coordination geometry of the Ir(III) atom is pseudo-octahedral. One of the chelate SiP ligands and one of the acetonitrile (Si1, P1, and N1) are located on one of the faces of the octahedron. The three remaining coordination sites are occupied by the other SiP ligand and MeCN (Si2, P2, and

https://doi.org/10.1021/acs.inorgchem.2c03953
Inorg. Chem. 2023, 62, 3095−3105

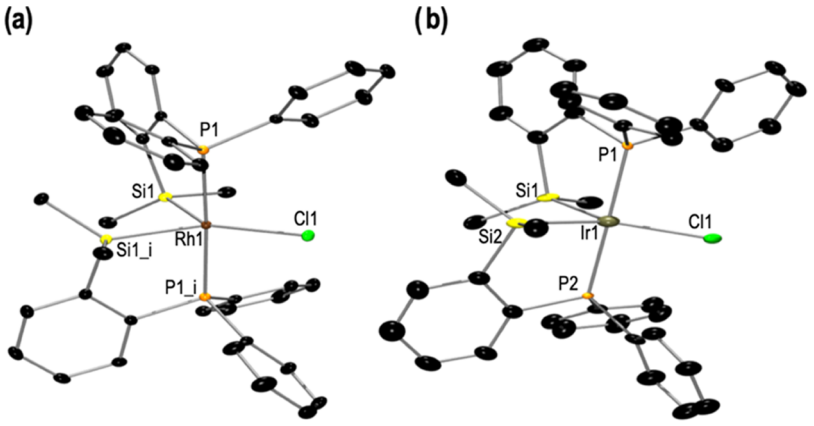

Figure 1. Displacement ellipsoids are drawn at a 50% probability level. The hydrogen atoms and solvent molecules are omitted for clarity. (a) Molecular structure of **1**. Selected bond lengths (Å) and angles (°): Rh1−Cl1 2.4357(8), Rh1−Si1 2.3099(6), Rh1−P1 2.3234(6), Si1−Rh1−Si1_i 83.37(3), P1−Rh1−P1_i 177.43(3), P1−Rh1−Si1 84.11(2), P1−Rh1−Cl1 91.28(2), and Si1−Rh1−Cl1 138.32(2). (b) Molecular structure of **2**. Selected bond lengths (Å) and angles (°): Ir1−Cl1 2.399(4), Ir1−P1 2.318(4), Ir1−P2 2.318(4), Ir1−Si1 2.319(5), Ir1−Si2 2.325(5), P1−Ir1−P2 178.25(15), Si1−Ir1−Si2 83.43(18), Si1−Ir1−P1 83.89(15), Si1−Ir1−P2 95.88(15), Si2−Ir1−P2 84.53(15), Si2−Ir1−P1 94.42(15), Si1−Ir1−Cl1 134.87(18), Si2−Ir1−Cl1 141.70(19), and P1−Ir1−Cl1 90.71(14), P2−Ir1−Cl1 90.17(14).

Scheme 3. Synthesis of Complexes 1[BAr$^F_4$] and 2[BAr$^F_4$]

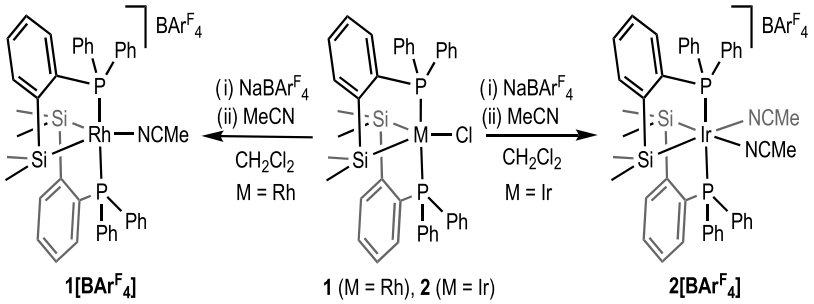

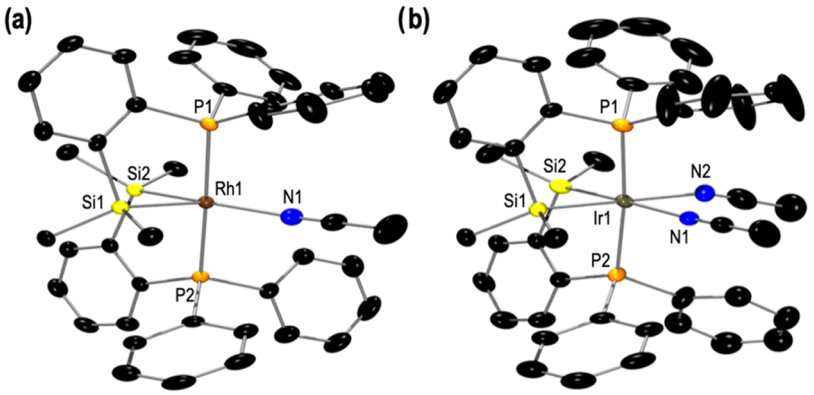

Figure 2. Displacement ellipsoids are drawn at a 50% probability level. The hydrogen atoms and the counteranion [BAr$^F_4$] are omitted for clarity. (a) Molecular structure of **1**[BAr$^F_4$]. Selected bond lengths (Å) and angles (°): Rh1−N1 2.163(3), Rh1−Si1 2.341(1), Rh1−Si2 2.311(1), Rh1−P1 2.317(1), Rh1−P2 2.317(1), Si1−Rh1−Si2 86.44(4), Si1−Rh1−N1 107.45(9), Si2−Rh1−N1 165.76(9). (b) Molecular structure of **2**[BAr$^F_4$]. Selected bond lengths (Å) and angles (°): Ir1−N1 2.279(4), Ir1−N2 2.148(3), Ir1−Si1 2.356(1), Ir1−Si2 2.366(1), Ir1−P1 2.331(1), Ir1−P2 2.326(1), Si1−Ir1−Si2 89.57(4), Si1−Ir1−N1 90.99(11), Si2−Ir1−N2 92.93(9), N1−Ir1−N2 86.52(14).

N2). The *trans*-labilizing nature of the silyl group is reflected in long Ir—N bond lengths [N1—Ir1 = 2.536(2) Å and N2—Ir1 = 2.536(2) Å], when compared with other iridium-acetonitrile distances in similar structures.[26]

Catalytic Hydrolysis of Diphenylsilane. Compounds, **1**, **2**, **1**[BAr$^F_4$], and **2**[BAr$^F_4$] were tested as precatalysts for the hydrolysis of Ph_2SiH_2 in tetrahydrofuran (THF) under standard reaction conditions (0.2 mol % catalyst, [Ph_2SiH_2] = 0.22 M, 10 equiv H_2O; see SI for more information). The H_2 evolution was monitored through the Man on the Moon X102 kit. The reaction profiles obtained (equiv of H_2 vs time) are shown in Figure 3.

It is worth highlighting the different reaction profiles obtained when comparing the cationic with the neutral compounds, which points to the integrity of the M−Cl bond through the catalytic process.

When Ir(III)-based catalysts **2** and **2**[BAr$^F_4$] were employed, more than 1.6 equiv of H_2 were liberated in the

https://doi.org/10.1021/acs.inorgchem.2c03953
Inorg. Chem. 2023, 62, 3095−3105

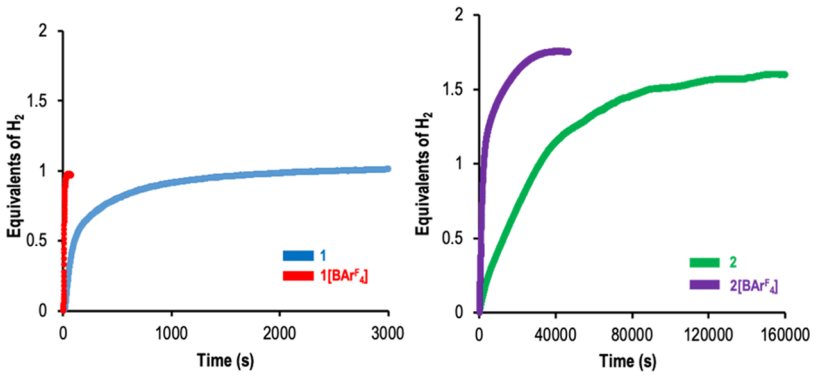

Figure 3. Reaction profiles (equiv of H_2 generated vs time) for hydrolysis of diphenylsilane using **1** and a **1**[$\mathbf{BAr^F_4}$] (left), **2** and **2**[$\mathbf{BAr^F_4}$] (right) as precatalysts. Reaction conditions: Silane (0.22 mmol), H_2O (2.2 mmol), 0.2 mol % of catalyst in 1 mL of THF at 25 °C under N_2. The hydrogen production was calculated by continuous monitoring of the pressure evolution using a pressure transducer (Man on the Moon X102 kit).

Table 1. Catalytic Hydrolysis of Diphenylsilane[a]

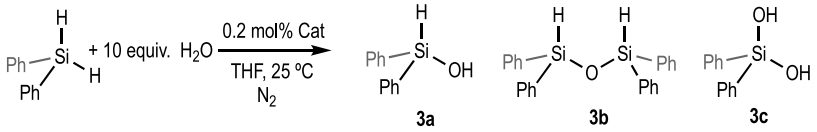

entry	cat.	H_2[b] equiv	time (s)	3a[c]	3b[c]	3c[c]
1	**1**	1	2500	93	7	
2	**2**	1.6	155,500			>99
3	**1**[$\mathbf{BAr^F_4}$]	1	50	1	99	
4	**2**[$\mathbf{BAr^F_4}$]	1.75	38,460			>99

[a]Reaction conditions: Silane (0.22 mmol), H_2O (2.2 mmol), 0.2 mol % of catalyst in 1 mL of THF at 25 °C. [b]Hydrogen equivalents evolved. [c]Molar ratio of products calculated by ^{1}H NMR.

process, being the product of the double hydrolysis, diphenylsilanediol (**3c** in Table 1, entries 2 and 4 and Figures S3 and S4 in SI), the only silane-containing product detected by ^{1}H NMR at the end of the reaction. Moreover, the absence of Ph_2SiH_2 indicates that the reaction is complete. In this process, the cationic **2**[$\mathbf{BAr^F_4}$] is more active than the neutral compound **2**. The reaction profiles observed, based on hydrogen evolution (Figure 3), did not show an evident two-stepped process, pointing to similar reaction rates for the first and second hydrolysis of the dihydrosilane.

To confirm the sequential formation of **3c**, the hydrolysis of diphenylsilane catalyzed by **2**[$\mathbf{BAr^F_4}$] was monitored by in situ ^{1}H NMR spectroscopy (Figure S5 in SI). The time-correlated speciation diagram obtained (Figure 4) shows the sigmoidal formation of diphenylsilanediol (**3c**), typical of consecutive reactions, being diphenylhydrosilanol (**3a**) the reaction intermediate. It is worth mentioning that the resemblance of the first and second hydrolysis rate constants hampers the isolation of diphenylhydrosilanol **3a** with Ir(III)-based catalyst **2** and **2**[$\mathbf{BAr_4^F}$].

In contrast, when the reaction was catalyzed by rhodium-(III)-based complexes **1** or **1**[$\mathbf{BAr^F_4}$], the reaction profile reached a plateau after liberating only 1 equiv of H_2 (Figure 3). The cationic complex **1**[$\mathbf{BAr^F_4}$] was the most efficient precatalyst, and the process was completed in only 50 seconds (Figure 3 and entry 3 in Table 1). When the neutral complex **1** was used as a precatalyst, 2500 s were required to reach the same conversion (Figure 3 and entry 1 in Table 1). The difference in reaction rate observed depending on the catalyst used (neutral or cationic) may be due to two reasons: (a) the easier accessibility of the substrate to the metal center in the case of the cationic complex; (b) the stronger electrophilicity of the cationic complexes with respect to the neutral ones.

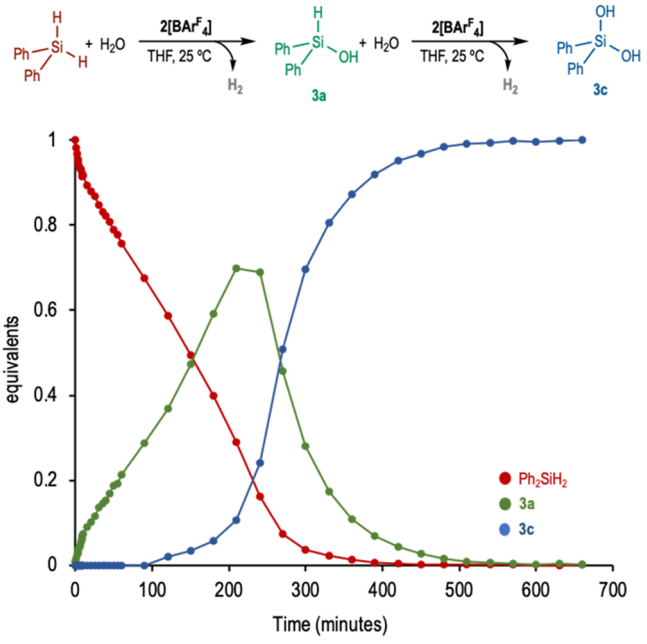

Figure 4. Time-correlated speciation diagram. Hydrolysis of Ph_2SiH_2 catalyzed by **2**[$\mathbf{BAr^F_4}$]. Reaction conditions: Ph_2SiH_2 (0.11 mmol), H_2O (1.1 mmol), **2**[$\mathbf{BAr^F_4}$] 0.2 mol %, 0.5 mL THF-d_8, 25 °C.

Surprisingly, ^{1}H NMR inspection of the reaction mixtures at the end of the reaction showed that the product obtained was mainly diphenylhydrosilanol (**3a**) when **1** was used as a

https://doi.org/10.1021/acs.inorgchem.2c03953
Inorg. Chem. 2023, 62, 3095−3105

catalyst (Table 1, entry 1 and Figure S1 in SI), but it proceeded toward tetraphenyldihydrosiloxane (**3b**) with the cationic catalyst **1**[BAr^F_4] (Table 1, entry 3 and Figure S2 in SI). Two reaction pathways can be envisaged for the formation of dihydrosiloxane **3b** under the reaction conditions: the condensation of two molecules of diphenylhydrosilanol (**3a**) (liberating one molecule of H_2O) or the nucleophilic attack of a diphenylhydrosilanol (**3a**) to a diphenyldihydrosilane (evolving 1 equiv of H_2) (Scheme 4).

Scheme 4. Possible Reaction Pathways for the Formation of Diphenyldihydrosiloxane Catalyzed by 1[BAr^F_4]

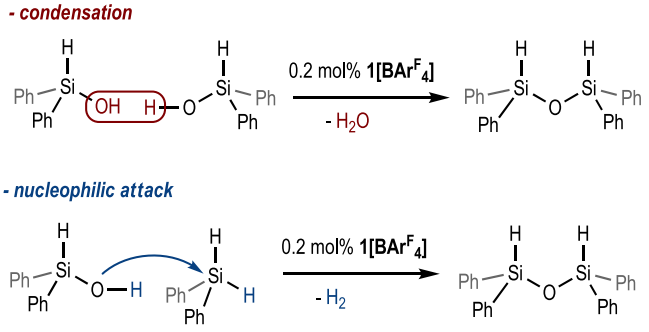

To shed some light on the origin of the observed dihydrosiloxane when using **1**[BAr^F_4], two control experiments were performed by means of ^{1}H NMR. First, diphenylhydrosilanol **3a** (0.11 mmol) was treated with 0.2 mol % of **1**[BAr^F_4] in THF-d_8 (0.5 mL) at 25 °C. The ^{1}H NMR spectrum acquired after 5 min of reaction shows nearly complete consumption of **3a** and the clear formation of the dihydrosiloxane **3b** (Scheme 5a, Figure S6a in SI). When an equimolecular mixture of diphenylhydrosilanol **3a** (0.11 mmol) and Ph_2SiH_2 (0.11 mmol) was reacted under identical conditions, the ^{1}H NMR spectra acquired after 5 min showed, as in the previous experiment, the formation of the dihydrosiloxane **3b** and the total consumption of **3a**. Noticeably, Ph_2SiH_2 was only partially (≈50%) consumed, which supports the hypothesis that **3b** is formed by a fast condensation of the formed diphenylhydrosilanol **3a**. The partial consumption of Ph_2SiH_2 must be attributed to its **1**[BAr^F_4]-catalyzed hydrolysis due to the H_2O formed during the condensation reaction. Accordingly, a small signal assigned to the H_2 generated in this process was observed in the ^{1}H NMR spectra (Scheme 5b and Figure S6b in SI).

The results obtained show that whereas both neutral and cationic rhodium complexes **1** and **1**[BAr^F_4] are very effective catalysts for the first hydrolysis of Ph_2SiH_2, in the case of **1**[BAr^F_4], the product of the reaction **3a** is immediately involved in a metal-mediated condensation process. Noticeably, this condensation reaction is not observed in the case of **1** at short reaction times. These results suggest the need of two coordination vacancies in the metal center, or a highly electrophilic metal center, for the condensation to proceed at competitive rates.

A global analysis of the results obtained with the four catalytic systems studied reveals the network of coexisting reactions in the hydrolysis of diphenylsilane (Scheme 6).[27] The different reaction rates for each individual step observed when compared to the different catalysts studied allowed us to selectively obtain the product of monohydrolysis (**3a**), its condensation product (**3b**), or the doubly hydrolyzed silane (**3c**). No other silane-containing products were detected by ^{1}H NMR in the reaction mixtures when iridium-based catalysts were used in the process, which discards the formation of polysiloxanes with these systems.

To confirm whether compound **1** at extended reaction times would catalyze the second hydrolysis or the condensation reaction, a catalytic reaction was conducted with this compound for 24 h. The reaction profile showed that after the initial formation of **3a**, a second equivalent of hydrogen evolved but at a much lower rate (Scheme 7 and Figure S7 in SI). ^{1}H NMR analysis of the final reaction mixture shows that the reaction product is not the diphenylsilanediol (**3c**), but a complex mixture of (O−$SiPh_2$−O) species (**3e** is proposed as one of these species, Figure S9 in SI). To obtain more information, the same reaction was monitored by in situ ^{1}H NMR spectroscopy (Figure S11 in SI). This experiment shows that after Ph_2SiH_2 is consumed, **3a** begins to transform into dihydrosiloxane **3b**, which subsequently transforms into another product containing at least one Si−H unit (probably **3d**). At longer reaction times, these signals evolve towards (O−$SiPh_2$−O) species. Similar results were obtained when the hydrolysis of Ph_2SiH_2 was conducted for 24 h with catalysts **1**[BAr^F_4] (Figures S8 and S10 in SI). Taken together, these results suggest that most probably, **1** follows a condensation route (*via* **3b**) rather than the double hydrolysis of the dihydrosilane (*via* **3c**) ($k_3 > k_2$).

Scheme 5. Control Experiments for Diphenyldihydrosiloxane Formation

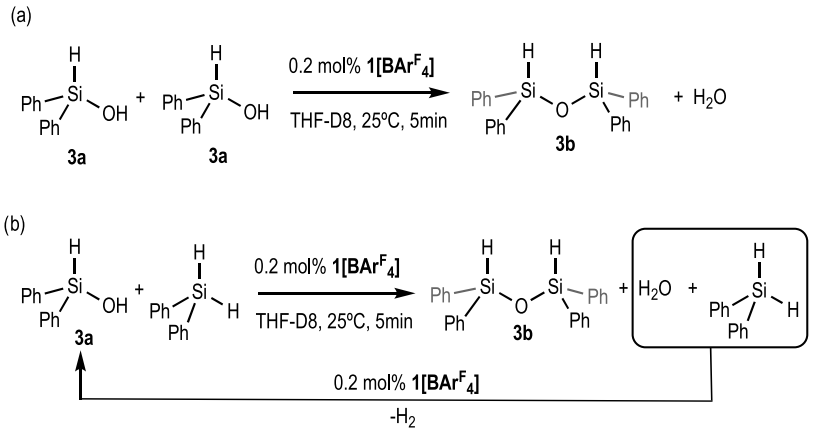

https://doi.org/10.1021/acs.inorgchem.2c03953
Inorg. Chem. 2023, 62, 3095−3105

Scheme 6. Hydrolysis of Diphenylsilane: Network of Potential Coexisting Reactions

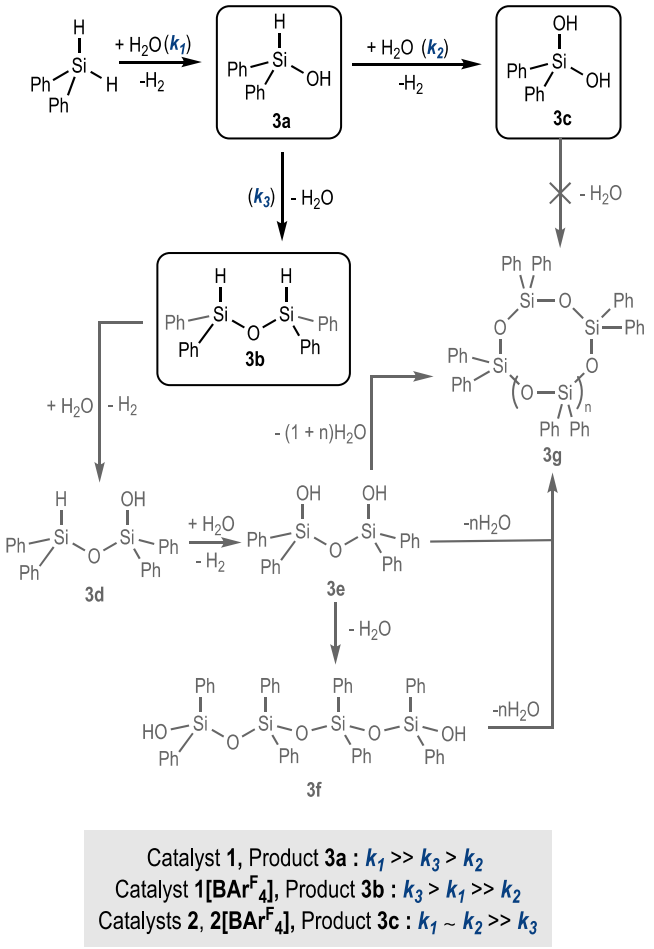

Hydrolysis of Other Secondary Silanes. The fine balance between rate constants observed when catalysts **1**, **1**[BAr^F_4], **2**, and **2**[BAr^F_4] were studied in the hydrolysis of Ph_2SiH_2 and the special relevance of hydrosilanols and hydrosiloxanes as valuable synthons for the chemical industry prompted us to extend the study of the rhodium-based catalysts to other commercial secondary silanes (entries 1−8 in Table 2).

The reaction of 1-naphtyl(phenyl)dihydrosilane (1-Naph(Ph)SiH_2) with H_2O in the presence of catalytic amounts of the rhodium complexes **1** or **1**[BAr^F_4] led to the formation of a mixture of hydrosilanol **3a′** and dihydrosiloxane **3b′** (entries 2 and 6 in Table 2), being the hydrosilanol **3a′** the main product (selectivity > 90%) in both cases. Accordingly, in both reactions, only 1 equiv of H_2 was released. As with Ph_2SiH_2, the reaction catalyzed by complex **1** was slower than the reaction catalyzed by **1**[BAr^F_4].

The results obtained in the hydrolysis of methyl(phenyl)-dihydrosilane (entries 3 and 7 of Table 2) show a change in the reactivity, obtaining the respective dihydrosiloxane **3b″** as a main product indistinctly when **1** or **1**[BAr^F_4] were used as precatalysts (selectivity > 90%). As with Ph_2SiH_2 and 1-Naph(Ph)SiH_2, these reactions only released 1 equiv of H_2 and the hydrolysis performed using the cationic rhodium complex is faster.

Finally, diethyldihydrosilane (Et_2SiH_2) was tested (entries 4 and 8 in Table 2). The hydrolysis of Et_2SiH_2 using **1** as a precatalyst releases 1 equiv of H_2, but the products formed could not be identified. Surprisingly, using this substrate and **1**[BAr^F_4] as a precatalyst, almost 2 equiv of H_2 were released, albeit at clearly different rates. The first equivalent was liberated in less than 1 min, and 25 min sufficed to reach completion. The product observed at the end of the reaction was diethylsilanediol (**3c‴**), presumably formed by hydrolysis of diethylhydrosilanol (**3a‴**).

The results obtained with the different silanes are compatible with the reaction scheme shown above (Scheme 6). Once the hydrosilanol is formed, its fate will depend on the relative rates of second hydrolysis (k_2) and condensation (k_3) reactions. If both are slow, the product could be isolated (as is the case with Ph_2SiH_2 and to a certain extent with 1-Naph(Ph)SiH_2). If the second hydrolysis is fast, the product will evolve to the corresponding silanediol (**C** in Table 2). The relative rates for the hydrolysis can be inferred from the calculated turnover frequency (TOFs) based on the liberation of 1 equiv of H_2. According to these values, this reaction is approximately 100 times faster using the cationic rhodium complex **1**[BAr^F_4] than when neutral **1** was used, with all the substrates. As discussed above, this enhanced reactivity toward the hydrolysis could be explained by the stronger electrophilicity and/or the better accessibility of the substrate to the catalytic pocket when the cationic catalyst is used. The relative reaction rates observed for the different substrates (Et_2SiH_2 > MePhSiH_2 > Ph_2SiH_2 > 1-Naph(Ph)SiH_2) support the important influence of electronic factors in the activation barrier for this process. This electronic effect could be extrapolated to the hydrolysis of the formed hydrosilanol. Consistently, only in the case of Et_2SiH_2, the diethylsilanediol (**3c‴**) was obtained. It is worth reminding that highly electrophilic Ir(III) catalyst **2** and **2**[BAr^F_4] were required to obtain the corresponding silanediol (**3c**) from Ph_2SiH_2.

Scheme 7. Hydrolysis of Diphenylsilane Catalyzed by 1 (a) and 1[BAr^F_4] (b) $TOFs_{1/2}$ Calculated in Red

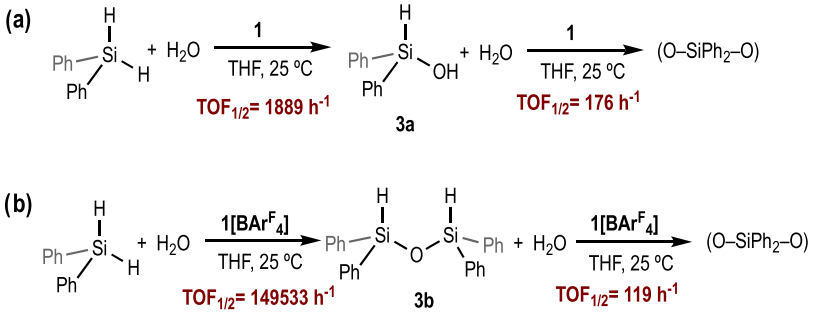

https://doi.org/10.1021/acs.inorgchem.2c03953
Inorg. Chem. 2023, 62, 3095−3105

Table 2. Catalytic Hydrolysis of Dihydrosilanes[a]

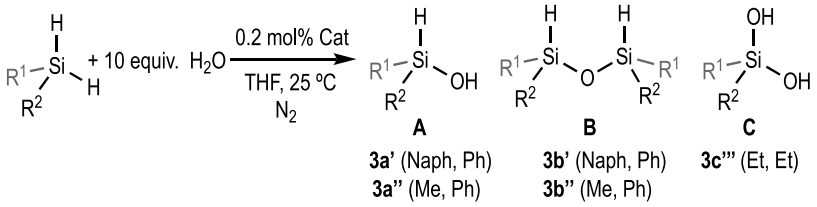

entry	cat.	R^1, R^2	H_2[b] equiv	$TOF_{1/2}$ (h^{-1})	A[c]	B[c]	C[c]
1	**1**	Ph, Ph	1	1889	93	7	
2	**1**	Ph, Naph	1	78	90	10	
3	**1**	Ph, Me	1	2991	10	90	
4	**1**	Et, Et	0.93	6452	unidentified		
5	**1**[BAr^F_4]	Ph, Ph	1	149,533	1	99	
6	**1**[BAr^F_4]	Ph, Naph	1	13,962	97	3	
7	**1**[BAr^F_4]	Ph, Me	1	472,861	2	98	
8	**1**[BAr^F_4]	Et, Et	1.8	390,087[d]			99

[a]Reaction conditions: Silane (0.22 mmol), H_2O (2.2 mmol), 0.2 mol % of catalyst in 1 mL of THF at 25 °C under N_2. [b]Hydrogen equivalents released. [c]Molar ratio of products calculated by ^1H NMR. [d]$TOF_{1/2}$ has been calculated for the release of 1 equiv of hydrogen.

Scheme 8. Gram-Scale Synthesis of Diphenylhydrosilanol and Diphenyldihydrosiloxane

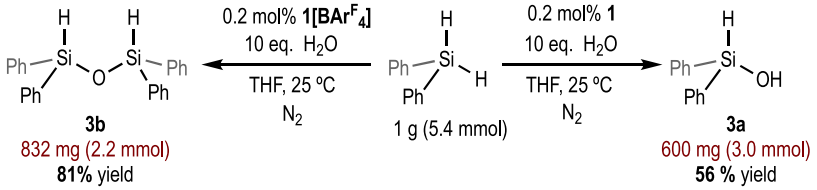

Alternatively, if the second hydrolysis is slow compared to the condensation reaction, the hydrosilanol could be isolated or evolve toward the dihydrosiloxane if involved in a fast metal-catalyzed condensation. According to the results obtained, steric effects determine the rate of the condensation process. When using the largest silane, 1-Naph(Ph)SiH_2, the major product obtained is unreacted hydrosilanol, independently of the catalyst used. In contrast, the product obtained when using Me(Ph)SiH_2 is the dihydrosiloxane.

In view of the excellent catalytic properties of our system, we decided to study the catalytic behavior of complex **1**[BAr^F_4] in the alcoholysis of Ph_2SiH_2 and the hydrolysis of other silanes (see Section S9 in SI). Satisfyingly, the alcoholysis of Ph_2SiH_2 with MeOH, EtOH, and iPrOH rendered the corresponding alkoxyhydrosilanes. When primary silanes were subjected to hydrolysis, the corresponding siloxanes were obtained as the main product, whereas tertiary silanes rendered an unidentified mixture of products liberating 2 equiv of H_2.

Scale-Up Experiments. It should be noted that, to the best of our knowledge, few efficient methods for the selective synthesis of hydrosilanols have been reported to date.[24]

To prove that using precataysts **1** and **1**[BAr^F_4], it is possible to obtain selectively the diphenylhydrosilanol (**3a**) and diphenyldihydrosiloxane (**3b**) in a gram-scale, the reaction of 5.4 mmol (1 g) of Ph_2SiH_2 with 10 equiv of H_2O under standard catalytic conditions (0.2 mol % of **1** or **1**[BAr^F_4] as catalyst, THF as solvent) was performed. When precatalyst **1** was used, this reaction led to the formation of diphenylhydrosilanol (**3a**) in a 56% of isolated yield (600 mg). Using **1**[BAr^F_4] as a precatalyst, diphenyldihydrosiloxane **3b** was obtained in 81% of isolated yield (832 mg) (Scheme 8).

The robustness of the catalytic system derived from **1**[BAr^F_4] was also confirmed through successive additions of Ph_2SiH_2. The sequential reaction profiles obtained showed that the catalyst maintained its activity for, at least, 10 successive cycles (Figure S12 in SI). In addition, in the case of the neutral compounds **1** and **2**, their structures remain unchanged after the catalytic reaction (Figures S1 and S3 in SI), which also demonstrate the robustness of the catalytic system.

CONCLUSIONS

In summary, two neutral {MCl[$SiMe_2$(*o*-$C_6H_4PPh_2$)]$_2$} (M = Rh, **1**; Ir, **2**) and two cationic {M[$SiMe_2$(*o*-$C_6H_4PPh_2$)]$_2$(NCMe)$_n$}[BAr^F_4] (M = Rh and *n* = 1, **1**[BAr^F_4]; M = Ir and *n* = 2, **2**[BAr^F_4]) complexes were prepared and structurally characterized in solution by NMR and in the solid state by X-ray crystallography. The four new complexes proved to be catalytically active in the hydrolysis of dihydrosilanes, rendering different products depending on the catalyst/substrate combination. These air-stable complexes have shown excellent catalytic properties with low catalyst loadings at room temperature and without the requirement of additives. A rational analysis of the different products obtained allowed us to propose a network of coexisting metal-catalyzed reactions of different nature (hydrolysis of hydrosilanes, condensation of silanols, and nucleophilic attack of silanols on hydrosilanes). Apparently, the latter are not operative with our systems. The results showed that hydrolytic processes are mainly controlled by the electronic nature of both catalysts and substrates, whereas metal-catalyzed condensations are mostly affected by sterics. This subtle balance permitted us to obtain selectively hydrosilanols, silanediols, or dihydrosilanes by an educated selection of the catalyst and substrate. The practical application of this methodology has been demonstrated by gram-scale synthesis experiments using Ph_2SiH_2.

https://doi.org/10.1021/acs.inorgchem.2c03953
Inorg. Chem. 2023, 62, 3095−3105

EXPERIMENTAL SECTION

General Considerations. The preparation of the metal complexes was carried out at room temperature under nitrogen by standard Schlenk techniques. Glassware was oven dried at 120 °C overnight and flamed under a vacuum prior to use. CH_2Cl_2 and THF were distilled over CaH_2 and Na, respectively, degassed by successive freeze−pump−thaw cycles and stored over molecular sieves (3 Å). $[RhCl(coe)_2]$[28] and $[IrCl(coe)_2]$[29] complexes and the proligand *o*-$Ph_2P(C_6H_4)SiMe_2H$[30] were prepared as previously reported. Microanalyses were carried out with a Leco CHNS-932 microanalyzer. NMR spectra were recorded with Bruker Avance DPX 300, Bruker Avance 400, or Bruker Avance 500 spectrometers at room temperature unless otherwise stated; ^1H and $^{13}C\{^1H\}$ (residual solvents) and $^{31}P\{^1H\}$ (H_3PO_4 external standard) spectra were measured from $CDCl_3$, CD_2Cl_2, THF-d_8 solutions. IR spectra were recorded with a Nicolet FTIR 510 spectrophotometer using KBr pellets.

*Synthesis of {MCl[SiMe$_2$(o-C$_6$H$_4$PPh$_2$)]$_2$} (M = Rh, **1**; M = Ir, **2**).* $[M(coe)_2Cl]_2$ (M = Rh, Ir) (0.14 mmol) was solved in CH_2Cl_2 (4 mL), 4 equiv of *o*-$Ph_2P(C_6H_4)SiMe_2H$ (180 mg, 0.560 mmol) were added, and it was stirred for 20 min. After this time, solvent was removed under the vacuum, and the resulting solid was washed with 5 mL of *n*-pentane and 5 mL of methanol and dried under vacuum to obtain a pale-yellow (**1**) and yellow (**2**) solids. Yield of **1** 164 mg (76%). Yield of **2** 201 mg (83%).

1. ^1H NMR (400 MHz, CD_2Cl_2): δ 8.10−7.10 (Si(*o*-$C_6H_4PPh_2$), 28 H_{arom}), −0.07 (s, Si−CH_3, 6H), −0.43 (s, Si−CH_3, 6H). $^{31}P\{^1H\}$ NMR (202 MHz CD_2Cl_2): δ 55.6 (d, $J_{Rh\text{-}P}$ = 120 Hz, 2P). $^{13}C\{^1H\}$ NMR (101 MHz, CD_2Cl_2): δ 160.0−128.0 (36 C_{arom}, Si(*o*-$C_6H_4PPh_2$)), 7.3 (s, 2C, Si−CH_3), 2.4 (s, 2C, Si−CH_3). Microanalysis ($RhClSi_2P_2C_{40}H_{40}\cdot CH_2Cl_2$): Requires: C 57.12, H 4.91. Obtained: C 56.95, H 5.02.

2. ^1H NMR (400 MHz, CD_2Cl_2): δ 8.02−7.25 (Si(*o*-$C_6H_4PPh_2$), 28 H_{arom}), −0.11 (s, Si−CH_3, 6H), −0.51 (s, Si−CH_3, 6H). $^{31}P\{^1H\}$ NMR (202 MHz, CD_2Cl_2): δ 54.4 (s, 2P). $^{13}C\{^1H\}$ NMR (101 MHz, CD_2Cl_2): δ 159.6−126.5 (36 C_{arom}, Si(*o*-$C_6H_4PPh_2$)), 5.5 (s, 2C, Si−CH_3), −0.3 (s, 2C, Si−CH_3). Microanalysis ($IrClSi_2P_2C_{40}H_{40}$): Requires: C 55.44, H 4.65. Obtained: C 55.55, H 4.58.

*Synthesis of {Rh[SiMe$_2$(o-C$_6$H$_4$PPh$_2$)]$_2$(NCMe)}[BAr^F$_4$] (**1[BAr^F$_4$]**) and {Ir[SiMe$_2$(o-C$_6$H$_4$PPh$_2$)]$_2$(NCMe)$_2$}[BAr^F$_4$] (**2[BAr^F$_4$]**).* To a Schlenk charged with the $[M(SiMe_2(o\text{-}C_6H_4PPh_2))_2Cl]$ (M = Rh, Ir) complex (**1**, 100 mg, 0.13 mmol; **2**, 112 mg, 0.13 mmol) and $NaBAr^F{}_4$ (127 mg, 0.14 mmol), 4 mL of CH_2Cl_2 was added. After 20 min stirring, the yellow suspension formed was filtered via cannula to remove NaCl. Addition of 1 mL of MeCN gave a pale-yellow solution, and it was left stirring 10 min. After this time, solvent was removed under vacuum to give a pale-yellow solid in both cases. Yield of **1**[$BAr^F{}_4$] 184 mg (86%). Yield of **2**[$BAr^F{}_4$] 194 mg (84%).

1[BAr^F$_4$]. ^1H NMR (400 MHz, $CDCl_3$): δ 7.73 (m, 8H, $BAr^F{}_4$), 7.55 (m, 4H, $BAr^F{}_4$), 7.70−7.32 (Si(*o*-$C_6H_4PPh_2$), 28 H_{arom}), 1.64 (s, CH_3−CN, 3H), 0.04 (s, Si−CH_3, 6H), −0.32 (s, Si−CH_3, 6H). $^{31}P\{^1H\}$ NMR (202 MHz, $CDCl_3$): δ 55.5 (d, $J_{Rh\text{-}P}$ = 120 Hz, 2P). $^{13}C\{^1H\}$ NMR (101 MHz, $CDCl_3$): δ 161.8 (q, $J_{B\text{-}C}$ = 50 Hz, $BAr^F{}_4$), 134.9 (s, $BAr^F{}_4$), 129.0 (q, $J_{F\text{-}C}$ = 12 Hz, $BAr^F{}_4$), 124.7 (q, $J_{F\text{-}C}$ = 273 Hz, CF_3), 122.4 (s, 2C, NC−CH_3), 117.6 (m, $BAr_4{}^F$), 159.0−128.0 (36 C_{arom}, Si(*o*-$C_6H_4PPh_2$)), 7.5 (s, 2C, Si−CH_3), 2.6 (s, 2C, Si−CH_3), 1.8 (s, 1C, NC−CH_3). Microanalysis ($RhSi_2P_2C_{74}H_{55}BNF_{24}$): Required: C 54.00, H 3.37, N 0.85. Obtained: C 53.88, H 3.55, N 1.02.

2[BAr^F$_4$]. ^1H NMR (400 MHz, $CDCl_3$): δ 7.71 (s, 8H, $BAr^F{}_4$), 7.53 (s, 4H, $BAr^F{}_4$), 7.75−7.70 (Si(*o*-$C_6H_4PPh_2$), 28 H_{arom}), 1.48 (s, CH_3−CN, 3H), −0.10 (s, Si−CH_3, 6H), −0.26 (s, Si−CH_3, 6H). $^{31}P\{^1H\}$ NMR (202 MHz, $CDCl_3$): δ 38.1 (s, 2P). $^{13}C\{^1H\}$ NMR (101 MHz, $CDCl_3$): δ 161.8 (q, $J_{B\text{-}C}$ = 50 Hz, $BAr^F{}_4$), 134.9 (s, $BAr^F{}_4$), 129.0 (q, $J_{F\text{-}C}$ = 12 Hz, $BAr_4{}^F$), 124.7 (q, $J_{F\text{-}C}$ = 273 Hz, CF_3), 119.3 (s, 2C, NC−CH_3), 117.6 (m, $BAr_4{}^F$), 160.0−127.0 (36 C_{arom}, Si(*o*-$C_6H_4PPh_2$)), 4.4 (s, 2C, Si−CH_3), 1.8 (s, 2C, NC−CH_3), 0.9 (s, 2C, Si−CH_3). Microanalysis ($IrSi_2P_2C_{76}H_{58}BN_2F_{24}$): Requires: C 51.39, H 3.29 N 1.58. Obtained: C 51.02, H 3.39, N 1.29.

X-ray Crystallography. Crystals for **1**, **1**[$BAr^F{}_4$], **2**, and **2**[$BAr^F{}_4$] were obtained by diffusion of pentane over CH_2Cl_2 and were mounted on a glass fiber and used for data collection on a Bruker Apex II with a photon detector equipped with graphite monochromated Mo Kα radiation (λ = 0.71073 Å). Lorentz-polarization and empirical absorption corrections were applied. The structures were solved by direct methods and refined with full-matrix least-squares calculations on F^2 using the program SHELXT.[31] Anisotropic temperature factors were assigned to all atoms except for hydrogen atoms, which are riding their parent atoms with an isotropic temperature factor arbitrarily chosen as 1.2 times that of the respective parent. Final $R(F)$, wR(F2), and goodness-of-fit agreement factors, details on the data collection, and analysis can be found in Table S1.

General Procedure for Catalytic Hydrolysis of Silanes. A closed reaction vessel equipped with a pressure transducer (Manonthemoon kinetic kit X102)[32] was immersed in a thermostated ethylene glycol/water bath and charged with the catalyst (0.00044 mmol) in 1 mL of distilled THF and H_2O (2.2 mmol). Once the pressure of the system was stabilized, the silane (0.22 mmol) was added, which was considered initial reaction time. The solution was left stirring until the pressure stabilized again, which was indicative that the reaction ended. The quantity of gas evolved was calculated from the measured pressure inside the reaction vessel following the ideal gases law equation (reactor volume 13.2 mL). Then, solvent was removed under vacuum, and the reaction mixture was analyzed by ^1H NMR to determine the molar ratio of products. The major reaction product was isolated through purification by column chromatography on silica gel using Hexane/EtOAc (10:1) as eluents.

*$Ph_2Si(H)OH$, Diphenylsilanol (**3a**).* ^1H NMR (400 MHz, $CDCl_3$): δ 7.68−7.63 (m, 4H_{arom}), 7.48−7.39 (m, 6H_{arom}), 5.53 (s, 1H, Si−H), 2.59 (s, 1H, Si−OH). $^{13}C\{^1H\}$ NMR (126 MHz, $CDCl_3$): δ 135.3 (2C), 134.3 (4C), 130.7 (2C), 128.4 (4C) ppm. HMQC ($^1H-^{29}Si$) NMR (400 MHz, $CDCl_3$): δ (^{29}Si) −12.9. IR (KBr): 3209 cm^{-1} (broad, Si−O−H), 2125 (Si−H) cm^{-1}.

*$Ph_2(H)SiOSi(H)Ph_2$, Tetraphenyldisiloxane (**3b**).* ^1H NMR (400 MHz, $CDCl_3$): δ 7.60−7.55 (m, 8H_{arom}), 7.45−7.40 (m, 4H_{arom}), 7.39−7.33 (m, 8H_{arom}), 5.62 (s, 2H, Si−H). $^{13}C\{^1H\}$ NMR (126 MHz, $CDCl_3$): δ 135.3 (4C), 134.7 (8C), 130.6 (4C), 128.3 (8C) ppm. HMQC ($^1H-^{29}Si$) NMR (400 MHz, $CDCl_3$): δ (^{29}Si) −19.5 ppm. Ir (KBr): 2123 cm^{-1} (Si−H), 1087 (Si−O−Si) cm^{-1}.

*$Ph_2Si(OH)_2$, Diphenylsilanediol (**3c**).* ^1H NMR (400 MHz, THF-d_8): δ 7.68−7.64 (m, 4H_{arom}), 7.32−7.23 (m, 6H_{arom}), 6.00 (s, 2H, Si−OH). $^{13}C\{^1H\}$ NMR (126 MHz, THF-d_8): δ 138.8 (2C), 135.2 (4C), 129.9 (2C), 128.0 (4C). HMQC ($^1H-^{29}Si$) NMR (400 MHz, THF-d_8): δ (^{29}Si) −33.3 ppm. IR (KBr): 3197 (broad, Si−O−H) cm^{-1}.

*1-NaphPhSi(H)OH, 1-Naphtyl(phenyl)silanol (**3a′**).* ^1H NMR (400 MHz, $CDCl_3$): δ 8.17 (dm, J = 7.9 Hz, 1H_{arom}), 7.97 (dm, J = 8.3 Hz, 1H_{arom}), 7.89 (tm, J = 7.5 Hz, 2H_{arom}), 7.68 (dm, J = 7.9 Hz, 2H_{arom}), 7.54−7.42 (m, 4H_{arom}), 7.39 (dm, J = 7.5 Hz, 2H_{arom}), 5.90 (s, 1H, Si−H), 2.80 (s, 1H, Si−OH). $^{13}C\{^1H\}$ NMR (126 MHz, $CDCl_3$): δ 137.1 (1C), 135.5 (1C), 135.4 (1C), 134.6 (2C), 133.6 (1C), 133.1 (1C), 131.5 (1C), 130.7 (1C), 129.2 (1C), 128.4 (2C), 128.1 (1C), 126.7 (1C), 126.1 (1C), 125.5 (1C). HMQC ($^1H-^{29}Si$) NMR (400 MHz, $CDCl_3$): δ (29Si) −13.2. IR (KBr): 3295 cm^{-1} (broad, Si−O−H), 2136 (Si−H) cm^{-1}.

*1-NaphPh(H)SiOSi(H)Ph(1-Naph), Di-1-naphtyl(diphenyl)-disiloxane (**3b′**).* ^1H NMR (400 MHz, $CDCl_3$): δ 8.06 (dd, J = 8.4 Hz, J = 4.0, 2H_{arom}), 7.95 (dd, J = 8.4 Hz, J = 4.0 Hz, 2H_{arom}), 7.87 (dd, J = 8.4 Hz, J = 3.2 Hz, 2H_{arom}), 7.84 (tm, J = 7.6 Hz, 2H_{arom}), 7.60 (tm, J = 7.6 Hz, 4H_{arom}), 7.49−7.40 (m, 6H_{arom}), 7.36−7.26 (m, 6H_{arom}), 6.00 (s, 2H, Si−H). $^{13}C\{^1H\}$ NMR (126 MHz, $CDCl_3$): δ 137.0 (2C), 135.6 (2C), 135.5 (2C), 134.5 (4C), 133.5 (2C), 133.0 (2C), 131.4 (2C), 130.5 (2C), 129.0 (2C), 128.3 (6C), 126.4 (2C), 126.0 (2C), 125.4 (2C). HMQC ($^1H-^{29}Si$) NMR (400 MHz, $CDCl_3$): δ (^{29}Si) −18.3 ppm. IR (KBr): 2129 cm^{-1} (Si−H), 1056 (Si−O−Si) cm^{-1}.

*MePh(H)SiOSi(H)PhMe, Dimethyl(diphenyl)disiloxane (**3b″**).* ^1H NMR (400 MHz, $CDCl_3$): δ 7.61−7.57 (m, 4H_{arom}), 7.44−7.37 (m,

https://doi.org/10.1021/acs.inorgchem.2c03953
Inorg. Chem. 2023, 62, 3095−3105

6H$_{arom}$), 5.18 (m, 2H, Si−H), 0.47 (d, J = 2.82 Hz, 6H, Si−CH$_3$). ^{13}C{^{1}H} NMR (126 MHz, CDCl$_3$): δ 137.4 (2C), 133.7 (4C), 130.2 (2C), 128.2 (4C), −0.3 (s, 2C, Si−CH$_3$). HMQC (^{1}H−^{29}Si) NMR (400 MHz, CDCl$_3$): δ (^{29}Si) −11.6. IR (KBr): 2132 cm^{-1} (Si−H), 1062 cm^{-1} (Si−O−Si).

*Et$_2$Si(OH)$_2$, Diethylsilanediol (**3c‴**).* ^{1}H NMR (400 MHz, THF-d$_8$): δ 4.96 (s, 2H, Si−OH), 0.93 (t, J = 7.9 Hz, 6H, CH$_3$) 0.45 (q, J = 7.9 Hz, 4H, CH$_2$). ^{13}C{^{1}H} NMR (126 MHz, THF-d$_8$): δ 7.5 (2C), 7.1 (2C). HMQC (^{1}H−^{29}Si) NMR (400 MHz, THF-d$_8$): δ (^{29}Si) −7.0. IR (KBr): 3162 cm^{-1} (broad, Si−O−H).

■ ASSOCIATED CONTENT

Supporting Information

The Supporting Information is available free of charge at https://pubs.acs.org/doi/10.1021/acs.inorgchem.2c03953.

Additional experimental details, NMR and FTRI spectra, and X-ray crystallographic tables (PDF)

Accession Codes

CCDC 2218418−2218421 contain the supplementary crystallographic data for this paper. These data can be obtained free of charge via www.ccdc.cam.ac.uk/data_request/cif, or by emailing data_request@ccdc.cam.ac.uk, or by contacting The Cambridge Crystallographic Data Centre, 12 Union Road, Cambridge CB2 1EZ, UK; fax: +44 1223 336033.

■ AUTHOR INFORMATION

Corresponding Authors

Zoraida Freixa − *Facultad de Química, Universidad del País Vasco (UPV/EHU), 20018 San Sebastián, Spain; IKERBASQUE, Basque Foundation for Science, 48011 Bilbao, Spain;* orcid.org/0000-0002-2044-2725; Email: zoraida_freixa@ehu.es

Miguel A. Huertos − *Facultad de Química, Universidad del País Vasco (UPV/EHU), 20018 San Sebastián, Spain; IKERBASQUE, Basque Foundation for Science, 48011 Bilbao, Spain;* orcid.org/0000-0002-5315-5642; Email: miguelangel.huertos@ehu.es

Authors

Unai Prieto-Pascual − *Facultad de Química, Universidad del País Vasco (UPV/EHU), 20018 San Sebastián, Spain*

Antonio Rodríguez-Diéguez − *Departamento de Química Inorgánica, Universidad de Granada, 18071 Granada, Spain;* orcid.org/0000-0003-3198-5378

Complete contact information is available at: https://pubs.acs.org/10.1021/acs.inorgchem.2c03953

Funding

The authors declare no competing financial interest.

Notes

The authors declare no competing financial interest.

■ ACKNOWLEDGMENTS

This publication is part of the projects PID2019-111281GB-I00 funded by MCIN/AEI/10.13039/501100011033, and IT1880-19, IT1741-22 and IT1553-22 founded by Gobierno Vasco. The authors thank SGiker for technical and human support. Universidad del Pais Vasco (to U.P.-P.) and IKERBASQUE (to M.A.H. and Z.F.) are acknowledged for personnel funding.

■ REFERENCES

(1) *Silicon-Containing Polymers: The Science and Technology of Their Synthesis and Applications*, Jones, R. G.; Ando, W.; Chojnowiski, J., Eds.; Kluwer Academic Publisher: London, 2000.

(2) *Advances in Silicones and Silicone-Modified Materials*, Clarson, S. J.; Owen, M. J.; Smith, S. D.; Van Dicke, M. E., Eds.; American Chemical Society: Washington, DC, 2010.

(3) Brook, M. A. *Silicon in Organic, Organometallic, and Polymer Chemistry*; Wiley & Sons: New York, 2000; pp 256−308.

(4) Marciniec, B.; Maciejewski, H.; Pietraszuk, C.; Pawluc, P. *Hydrosilylation: A Comprehensive Review on Recent Adavances*; Springer: Berlin, 2009.

(5) For recent reviews in hydrosilylation reactions see for example: (a) Sun, J.; Deng, L. Cobalt complex-catalyzed hydrosilylation of alkenes and alkynes. *ACS Catal.* **2016**, *6*, 290−300. (b) Du, X.; Huang, Z. Advances in base-metal-catalyzed alkene hydrosilylation. *ACS Catal.* **2017**, *7*, 1227−1243. (c) Zaranek, M.; Pawluc, P. Markovnikov hydrosilylation of alkenes: how an oddity becomes de goal. *ACS Catal.* **2018**, *8*, 9865−9876. (d) Yang, X.; Wang, C. Manganese-catalyzed hydrosilylation reactions. *Chem. - Asian J.* **2018**, *13*, 2307−2315. (e) Obligacion, J. V.; Chirick, P. J. Earth-abundant transition metal catalysts for alkene hydrosilylation and hydroboration. *Nat. Rev. Chem.* **2018**, *2*, 15−34. (f) Raya-Barón, A.; Oña-Burgos, P.; Fernández, I. Iron catalyzed homogeneous hydrosilylstion of ketones and aldehydes: advances and mechanistic perspective. *ACS Cat.* **2019**, *9*, 5400−5417. (g) Uvarov, V. M.; Vekki, D. A. Recent progress in the development of catañytic system for homogeneous asymmetric hydrosilylation of ketones. *J. Organomet. Chem.* **2020**, *923*, 121415. (h) Bhunia, M.; Sreejyothi, P.; Mandal, K. Earth-abundant metal catalyzed hydrosilylative reduction of various functional groups. *Coord. Chem. Rev.* **2020**, *405*, 213110. (i) Naganawa, Y.; Inomata, K.; Sato, K.; Nakajima, Y. Hydrosilylation reactions of functionalized alkenes. *Tetrahedron Lett.* **2020**, *61*, 151513. (j) Almeida, L. D.; Wang, H.; Junge, K.; Cui, X.; Beller, M. Recent advances in catalytic hydrosilylations: developments beyond traditional platinum catalysts. *Angew. Chem., Int. Ed.* **2021**, *60*, 550−565.

(6) (a) Cheng, C.; Simmons, E. M.; Hartwig, J. F. Iridium-catalyzed, diastereoselective dehydrogenative silylation of terminal alkenes with (TMSO)$_2$MeSiH. *Angew. Chem., Int. Ed.* **2013**, *52*, 8984−8989. (b) Cheng, C.; Hartwig, J. F. Rhodium-catalyzed intermolecular C-H silylation of arenes with high steric regiocontrol. *Science* **2014**, *343*, 853−857. (c) Mei, J.; Kim, D. H.; Ayzner, A. L.; Toney, M. F.; Bao, Z. Siloxane-terminated solubilizing side chains: bringing conjugated polymer backbones closer and boosting hole mobilities in thin-film transistors. *J. Am. Chem. Soc.* **2011**, *133*, 20130−20133. (d) Schwartz, G.; Tee, B. C.-K.; Mei, J.; Appleton, A. L.; Kim, D. H.; Wang, H.; Bao, Z. Flexible polymer transistors with high pressure sensitivity for applications in electronic skin and health monitoring. *Nat. Commun.* **2013**, *4*, No. 1859. (e) Brząkalski, D.; Walczak, M.; Duszczak, J.; Dudziec, B.; Marciniec, B. Chlorine-Free Catalytic Formation of Silsesquioxanes with Si-OH and Si-OR Functional Groups. *Eur. J. Inorg. Chem.* **2018**, *2018*, 4905−4910.

(7) (a) Murugavel, R.; Voigt, A.; Walawalkar, M. G.; Roesky, H. W. Hetero- and metallasiloxanes derived from silanediols, disilanols, silanetriols and trisilanols. *Chem. Rev.* **1996**, *96*, 2205−2236. (b) Li, G.; Wang, L.; Ni, H.; Pittman, C. U., Jr. Polyhedral oligomeric silsesquioxane (POSS) polymers and copolymers: A review. *J. Inorg. Organomet. Polym.* **2001**, *11*, 123−154.

(8) Denmark, S. E.; Regens, C. S. Palladium-catalyzed cross-coupling reactions of organosilanols and their salts: practical alternatives to boron- and tin-based methods. *Acc. Chem. Res.* **2008**, *41*, 1486−1499.

(9) Wakabayashi, R.; Kawahara, K.; Kuroda, K. Nonhydrolytic Synthesis of Branched Alkoxysiloxane Oligomers Si[OSiH(OR)$_2$]$_4$ (R= Me, Et). *Angew. Chem., Int. Ed.* **2010**, *49*, 5273−5277.

(10) Satoh, Y.; Igarashi, M.; Sato, K.; Shimada, S. Highly selective synthesis of hydrosiloxanes by Au-catalyzed dehydrogenative cross-coupling reaction of silanols with hydrosilanes. *ACS Catal.* **2017**, *7*, 1836−1840.

(11) Pattanaik, S.; Gunanathan, C. Cobalt-catalyzed selective synthesis of hydrodisiloxanes. *ACS Catal.* **2019**, *9*, 5552−5561.
(12) Takeshita, T.; Sato, K.; Nakajima, Y. Selective hydrosiloxane synthesis via dehydrogenative coupling of silanols with hydrosilanes catalyzed by Fe complexes bearing a tetradentate PNNP ligand. *Dalton Trans.* **2018**, *47*, 17004−17010.
(13) (a) Le Coz, E.; Kahlal, S.; Saillard, J.-Y.; Roisnel, T.; Dorcet, V.; Carpentier, J-F.; Sarazin, Y. Barium Siloxides and Catalysed Formation of Si-O-Si' Motifs. *Chem. - Eur. J.* **2019**, *25*, 13509−13513. (b) Kuciński, K.; Stachowiak, H.; Hreczycho, G. Silylation of silanols with hydrosilanes via main group catalysis: the synthesis of unsymmetrical siloxanes and hydrosiloxanes. *Inorg. Chem. Front.* **2020**, *7*, 4190−4196.
(14) Satoh, Y.; Fuchise, K.; Nozawa, T.; Sato, K.; Igarashi, M. A catalyst- and additive-free synthesis of alkoxyhydrosiloxanes from silanols and alkoxyhydrosilanes. *Chem. Commun.* **2020**, *56*, 8218−8221.
(15) (a) Chandrasekhar, V.; Boomishankar, R.; Nagendran, S. Recent Developments in the Synthesis and Structure of Organosilanols. *Chem. Rev.* **2004**, *104*, 5847−5910. (b) Jeon, M.; Han, J.; Park, J. Catalytic Synthesis of Silanols from Hydrosilanes and Applications. *ACS Catal.* **2012**, *2*, 1539−1549.
(16) Cella, J. A.; Carpenter, J. C. Procedures for the preparation of silanols. *J. Organomet. Chem.* **1994**, *480*, 23−26.
(17) (a) Lickiss, P. D.; Lucas, R. Oxidation of Sterically Hindered Organosilicon Hydrides Using Potassium Permanganate. *J. Organomet. Chem.* **1996**, *521*, 229−234. (b) Valliant-Saunders, K.; Gunn, E.; Shelton, G. R.; Hrovat, D. A.; Borden, W. T.; Mayer, J. M. Oxidation of Tertiary Silanes by Osmium Tetroxide. *Inorg. Chem.* **2007**, *46*, 5212−5219. (c) Adam, W.; Mello, R.; Curci, R. O-Atom Insertion into Si-H Bonds by Dioxiranes: A Stereospecific and Direct Conversion of Silanes into Silanols. *Angew. Chem., Int. Ed.* **1990**, *29*, 890−891. (d) Spialter, L.; Pazdernik, L.; Bernstein, S.; Swansiger, W. A.; Buell, G. R.; Freeburger, M. E. Mechanism of The Reaction of Ozone with The Silicon-hydrogen Bond. *J. Am. Chem. Soc.* **1971**, *93*, 5682−5686.
(18) (a) Adam, W.; Garcia, H.; Mitchell, C. M.; Saha-Moller, C. R.; Weichold, O. The Selective Catalytic Oxidation of Silanes to Silanols with H_2O_2 activated by the Ti-beta Zeolite. *Chem. Commun.* **1998**, 2609−2610. (b) Adam, W.; Mitchell, C. M.; Saha-Moller, C. R.; Weichold, O. Host−Guest Chemistry in a Urea Matrix: Catalytic and Selective Oxidation of Triorganosilanes to the Corresponding Silanols by Methyltrioxo- rhenium and the Urea/Hydrogen Peroxide Adduct. *J. Am. Chem. Soc.* **1999**, *121*, 2097−2103. (c) Ishimoto, R.; Kamata, K.; Mizuno, N. Highly Selective Oxidation of Organo- silanes to Silanols with Hydrogen Peroxide Catalyzed by a Lacunary Polyoxotungstate. *Angew. Chem., Int. Ed.* **2009**, *48*, 8900−8904. (d) Wang, K.; Zhou, J.; Jiang, Y.; Zhang, M.; Wang, C.; Xue, D.; Tang, W.; Sun, H.; Xiao, J.; Li, C. Selective Manganese-Catalyzed Oxidation of Hydrosilanes to Silanols under Neutral Reaction Conditions. *Angew. Chem., Int. Ed.* **2019**, *58*, 6380−6384.
(19) Okada, Y.; Oba, M.; Arai, A.; Tanaka, K.; Nishiyama, K.; Ando, W. Diorganotelluride-Catalyzed Oxidation of Silanes to Silanols under Atmospheric Oxygen. *Inorg. Chem.* **2010**, *49*, 383−385.
(20) (a) Asao, N.; Ishikawa, Y.; Hatakeyama, N.; Menggenbateer; Yamamoto, Y.; Chen, M.; Zhang, W.; Inoue, A. Nanostructured materials as catalysts: nanoporous-gold-catalyzed oxidation of organosilanes with water. *Angew. Chem., Int. Ed.* **2010**, *49*, 10093−10095. (b) John, J.; Gravel, E.; Hagege, A.; Li, H.; Gacoin, T.; Doris, E. Catalytic oxidation of silanes by carbon nanotube-gold nanohybrids. *Angew. Chem., Int. Ed.* **2011**, *50*, 7533−7536. (c) Liang Teo, A. K.; Fan, W. Y. A novel iron complex for highly efficient catalytic hydrogen generation from the hydrolysis of organosilanes. *Chem. Commun.* **2014**, *50*, 7191−7194. (d) Lee, M.; Ko, S.; Chang, S. Highly selective and practical hydrolytic oxidation of organosilanes to silanols catalyzed by a ruthenium complex. *J. Am. Chem. Soc.* **2000**, *122*, 12011−12012. (e) Tan, S.; Kee, J. W.; Fan, W. Y. Catalytic hydrone generation from the hydrolysis of silanes by ruthenium complexes. *Organometallics* **2011**, *30*, 4008−4013. (f) Ison, E. A.; Corbin, R. A.; Abu-Omar, M. M. Hydrogen Production from Hydrolytic Oxidation of Organosilanes Using a Cationic Oxorhenuim Catalyst. *J. Am. Chem. Soc.* **2005**, *127*, 11938−11939. (g) Corbin, R. A.; Ison, E. A.; Abu-Omar, M. M. Catalysis by cationic oxorhenium(V): hydrolysis and alcoholysis of organic silanes. *Dalton Trans.* **2009**, 2850−2855. (h) Krüger, A.; Albrecht, M. Rhodium Carbene Complexes as Versatile Catalyst Precursor for Si−H Bond Activation. *Chem. - Eur. J.* **2012**, *18*, 652−658. (j) Lee, Y.; Seomoon, D.; Kim, S.; Han, H.; Chang, S.; Lee, P. H. Highly Efficient Iridium-Catalyzed Oxidation of Organosilanes to Silanols. *J. Org. Chem.* **2004**, *69*, 1741−1743. (k) Garcés, K.; Fernandez-Alvarez, F. J.; Polo, V.; Lalrempuia, R.; Perez-Torrente, J. J.; Oro, L. A. Iridium-Catalyzed Hydrogen Production from Hydrosilanes and Water. *ChemCatChem* **2014**, *6*, 1691−1697. (l) Aliaga-Lavrijsen, M.; Iglesias, M.; Cebollada, A.; Garces, K.; Garcia, N.; Sanz Miguel, P. J.; Fernandez-Alvarez, F. J.; Perez-Torrente, J. J.; Oro, L. A. Hydrolysis and Methanolysis of Silanes Catalyzed by Iridium(III) Bis-N-Hetrocyclic Carbene Complex: Influence of the Wingtip Groups. *Organometallics* **2015**, *34*, 2378−2385. (m) Wang, Y.; Lu, J.; Ma, X.; Niu, Y.; Singh, V.; Ma, P.; Zhang, C.; Niu, J.; Wang, J. Synthesis, characterization and catalytic oxidation of organosilanes with a novel multilayer polyoxomolybdate containing mixed-valence antimony. *Mol. Catal.* **2018**, *452*, 167−174. (n) Yu, M.; Jing, H.; Fu, X. Highly efficient generation of hydrogen from the hydrolysis of silanes catalyzed by $[RhCl(CO)_2]_2$. *Inorg. Chem.* **2013**, *52*, 10741−10743. (o) Almenara, N.; Garralda, M. A.; Lopez, X.; Matxain, J. M.; Freixa, Z.; Huertos, M. A. Hydrogen Tunneling in Catalytic Hydrolysis and Alcoholysis of Silanes. *Angew. Chem., Int. Ed.* **2022**, *61*, No. e202204558.
(21) (a) Mitsudome, T.; Arita, S.; Mori, H.; Mizugaki, T.; Jitsukawa, K.; Kaneda, K. Supported Silver-Nanoparticle-Catalyzed Highly Efficient Aqueous Oxidation of Phenylsilanes to Silanols. *Angew. Chem., Int. Ed.* **2008**, *47*, 7938−7940. (b) Mitsudome, T.; Noujima, A.; Mizugaki, T.; Jitsukawa, K.; Kaneda, K. Supported gold nanoparticle catalyst for the selective oxidation of silanes to silanols in water. *Chem. Commun.* **2009**, 5302−5304. (c) Asao, N.; Ishikawa, Y.; Hatakeyama, N.; Menggenbateera; Yamamoto, Y.; Chen, M.; Zhang, W.; Inoue, A. Nanostructures Materials as Catalysts: Nanoporous-Gold-Catalyzed Oxidation of Organosilanes with Water. *Angew. Chem., Int. Ed.* **2010**, *49*, 10093−10095. (d) John, J.; Gravel, E.; Hagège, A.; Li, H.; Gacoin, T.; Doris, E. Catalytic Oxidation of Silanes by Carbon Nanotube-Gold Nanohybrids. *Angew. Chem., Int. Ed.* **2011**, *50*, 7533−7536. (e) Shimizu, K.-i.; Kubo, T.; Satsuma, A. Surface Oxygen-Assisted Pd Nanoparticle Catalysis for Selective Oxidation of Silanes to Silanols. *Chem. - Eur. J.* **2012**, *18*, 2226−2229. (f) Jeon, M.; Han, J.; Park, J. Transformation of Silanes into Silanols using Water and Recyclable Metal Nanoparticle Catalyst. *ChemCatChem* **2012**, *4*, 521−524.
(22) Liang, H.; Wang, L.-J.; Ji, Y.-X.; Wang, H.; Zhang, B. Selective Electrochemical Hydrolysis of Hydrosilanes to Silanols via Anodically Generated Silyl Cations. *Angew. Chem., Int Ed.* **2021**, *60*, 1839−1844.
(23) Bähr, S.; Brinkman-Chen, S.; Garcia-Borrás, M.; Roberts, J. M.; Katsoulis, D. E.; Houk, K. N.; Arnold, F. H. Selective Enzymatic Oxidation of Silanes to Silanols. *Angew. Chem., Int. Ed.* **2020**, *132*, 15637−15641.
(24) (a) Tsuchido, Y.; Kanda, K.; Osakada, K. Gold(I) complexes with chloro(diaryl)silyl ligand. Stoichiometric reactions and catalysis for O-functionalization of organosilane. *Tetrahedron* **2020**, *76*, 131076. (b) Yuan, W.; Zhu, X.; Xu, Y.; He, C. Synthesis of Si-Stereogenic Silanols by Catalytic Asymmetric Hydrolytic Oxidation. *Angew. Chem., Int. Ed.* **2022**, *61*, No. e202204912.
(25) (a) Auburn, M. J.; Stobart, S. R. (phosphinoalkyl)silyl complexes. 5. Synthesis and reactivity of congeneric chelate-stabilized disilyl complexes of rhodium(III) and iridium(III): chlorobis-[[(diphenylphosphino)ethyl]dimethylsilyl]rhodium and -iridium. *Inorg. Chem.* **1985**, *24*, 318−323. (b) Azpeitia, S.; Fernandez, B.; Garralda, M. A.; Huertos, M. A. Silyl−Thioether Multidentate Ligands: Synthesis of Rh(III) Complexes via Rh(I)/Rh(III) Mixed-Valent and Cyclooctenyl Intermediates. *Eur. J. Inorg. Chem.* **2015**, *2015*, 5451−5456.

https://doi.org/10.1021/acs.inorgchem.2c03953
Inorg. Chem. 2023, 62, 3095−3105

(26) McGee, K. A.; Mann, K. R. Selective low-temperature synthesis of facial and meridional tris-cyclometalated iridium(III) complexes. *Inorg. Chem.* **2007**, *46*, 7800−7809.
(27) The evolution from dihydrosiloxane to polysiloxane products has been inferred considering reaction pathways involving hydrolysis of hydrosilane derivatives and condensation reactions of polysiloxanols. Possible paths involving nucleophilic attack of silanols on hydrosilanes have been discarded based on the lack of reactivity of diphenyldihydrosilane and diphenylhydrosilanol observed with catalyst **1**[$\mathbf{BAr_4^F}$], but a full picture considering also these reaction paths is presented in Figure S25.
(28) Bennet, M. A.; Saxby, J. D. Cyclooctatetraene-Rhodium(I) Complexes. *Inorg. Chem.* **1967**, *7*, 321−324.
(29) Herde, J. L.; Senoff, C. V. μ-Dichlorotetrakis(cyclooctene) diriidium(I). *Inorg. Nucl. Chem. Lett.* **1971**, *7*, 1029.
(30) Zhang, F.; Wang, L.; Chang, S.-H.; Huang, K.-L.; Chi, Y.; Hung, W.-Y.; Chen, C.-M.; Lee, G.-H.; Chou, P.-T. Phosphorescent Ir(III) complexes with both cyclometalate chromophores and phosphine-silanolate ancillary: concurrent conversion of organosilane to silanolate. *Dalton Trans.* **2013**, *42*, 7111−7119.
(31) Sheldrick, G. M. Integrated space-group and crystal-structure determination. *Acta Crystallogr., Sect. A: Found. Adv.* **2015**, *71*, 3−8.
(32) www.manonthemoontech.com. For recent examples using this setup see www.manonthemoontech.com/news.html.

https://doi.org/10.1021/acs.inorgchem.2c03953
Inorg. Chem. 2023, 62, 3095−3105